

See discussions, stats, and author profiles for this publication at: <https://www.researchgate.net/publication/10900568>

Transferred Nuclear Overhauser Effect in Nuclear Magnetic Resonance Diffusion Measurements of Ligand–Protein Binding

ARTICLE *in* ANALYTICAL CHEMISTRY · MARCH 2003

Impact Factor: 5.64 · DOI: 10.1021/ac020563o · Source: PubMed

CITATIONS

26

READS

23

5 AUTHORS, INCLUDING:



Jiangli Yan

Pfizer Inc.

27 PUBLICATIONS 686 CITATIONS

SEE PROFILE



Cynthia K Larive

University of California, Riverside

180 PUBLICATIONS 3,681 CITATIONS

SEE PROFILE



Michael J Shapiro

Pfizer Inc.

126 PUBLICATIONS 3,460 CITATIONS

SEE PROFILE

Transferred Nuclear Overhauser Effect in Nuclear Magnetic Resonance Diffusion Measurements of Ligand–Protein Binding

Laura H. Lucas,[†] Jiangli Yan,[‡] Cynthia K. Larive,^{*,†} Edward R. Zartler,[‡] and Michael J. Shapiro[‡]

Department of Chemistry, University of Kansas, Lawrence, Kansas 66045, and Lilly Research Laboratories, Eli Lilly and Company, Indianapolis, Indiana 46285

The drug discovery process relies on characterizing structure–activity relationships, since specific ligand–target interactions often result in important biological functions. Measuring diffusion coefficients by nuclear magnetic resonance spectroscopy is a useful way to study binding, because changes can be detected when a small ligand interacts with a macromolecular target. Diffusion coefficients can be miscalculated, however, due to magnetization transfer between the receptor and ligand. This transferred nuclear Overhauser effect (trNOE) disrupts the observed signal decay due to diffusion as a function of the experimental diffusion time. Since longer diffusion times also selectively edit free ligand signal, the measured diffusion coefficients become biased toward the fraction of bound ligand. Despite this discrepancy, under these experimental conditions, the trNOE selectively influences the measured signals of binding ligands and can be used to gain insight into ligand–protein interactions. These phenomena have been studied for caffeine and L-tryptophan, which bind to human serum albumin, and the antimalarial agent trimethoprim, which interacts with dihydrofolate reductase. The results provide insight into the nature of ligand–protein binding and are thus useful for elucidating the molecular features of the ligand that interact with the protein.

Nuclear magnetic resonance (NMR) screening in drug discovery depends on robust techniques that efficiently reveal lead molecules. The molecular interactions of a lead molecule with its target or a nontarget protein, e.g., human serum albumin (HSA), must be characterized to determine efficacy and potential side effects. The effects of ligand scaffold modifications on biological activity can be described quantitatively and in unbiased equilibrium conditions by probing structure–activity relationships (SAR) with spectroscopic methods such as NMR.¹ Diffusion measurements made by NMR have been used to characterize a variety of molecular interactions,^{2–4} and in recent years, much attention has

been directed to a subset of diffusion-based techniques known as “affinity NMR” because of their applicability to drug screening.⁵ These techniques are frequently used to analyze ligand–receptor binding and thus provide a means for assessing molecular interactions that can either reduce bioavailability or induce a desired biological response.^{6,7}

The typical diffusion experiment uses bipolar gradient pulse pairs⁸ such as those shown in the bipolar pulse pair stimulated echo (BPPSTE) pulse sequence shown in Figure 1A. The first pair of gradient pulses spatially encode the nuclear spins of molecules, whether protein or ligand, according to their physical positions within the NMR detection coil. After a delay time, Δ , during which diffusion occurs, the spins are decoded with a second set of identical gradient pulses. Diffusion from the original encoding position results in attenuated signal. Translational diffusion coefficients are calculated from this signal attenuation monitored as a function of the applied magnetic field gradient amplitude (g , for a rectangular pulse) according to eq 1,^{9,10} where

$$I = I_0 \exp[-D(\delta\gamma g)^2(\Delta - \delta/3 - \tau/2)] \quad (1)$$

I is the resonance intensity measured for a given gradient amplitude, I_0 is the intensity in the absence of the gradient pulse, γ is the gyromagnetic ratio, δ is the duration of the bipolar gradient pulse pair, Δ is the diffusion delay time, and τ is a short gradient recovery delay during which relaxation and spin–spin coupling evolution are not significant. As shown in Figure 1A, sine bell-shaped gradient pulses can also be used (g'), where the effective gradient amplitude is scaled by a factor of $2/\pi$ relative to the rectangular pulse.¹¹

For ligand–protein systems with $K_d > 1 \mu\text{M}$, the ligands are in fast chemical exchange between bound and free states.

- (4) Waldeck, A. R.; Kuchel, P. W.; Lennon, A. J.; Chapman, B. E. *Prog. Nucl. Magn. Reson. Spectrosc.* **1997**, *30*, 39–68.
- (5) Chen, A.; Shapiro, M. J. *Anal. Chem.* **1999**, *71*, 669A–675A.
- (6) Shapiro, M. J.; Wareing, J. R. *Curr. Opin. Drug Discovery Dev.* **1999**, *2*, 396–400.
- (7) Lin, M.; Shapiro, M. J.; Wareing, J. R. *J. Org. Chem.* **1997**, *62*, 8930–8931.
- (8) Wu, D.; Chen, A.; Johnson, C. S., Jr. *J. Magn. Reson., Ser. A* **1995**, *115*, 260–264.
- (9) Price, W. S. *Concepts Magn. Reson.* **1997**, *9*, 299–336.
- (10) Price, W. S. *Concepts Magn. Reson.* **1998**, *10*, 197–237.
- (11) Kohlmann, O.; Steinmetz, W. E.; Mao, X.; Wuelfing, P.; Templeton, A. C.; Murray, R. W.; Johnson, C. S., Jr. *J. Phys. Chem. B* **2001**, *105*, 8801–8809.

* To whom correspondence should be addressed: (e-mail) clarive@ku.edu.

[†] University of Kansas.

[‡] Eli Lilly and Co.

- (1) Shuker, S. B.; Hajduk, P. J.; Meadows, R. P.; Fesik, S. W. *Science* **1996**, *274*, 1531–1534.
- (2) Zimmerman, J. R.; Brittin, W. E. *J. Phys. Chem.* **1957**, *61*, 1328–1333.
- (3) Kärger, J.; Pfeifer, H.; Heink, W. *Adv. Magn. Reson.* **1988**, *12*, 1–89.

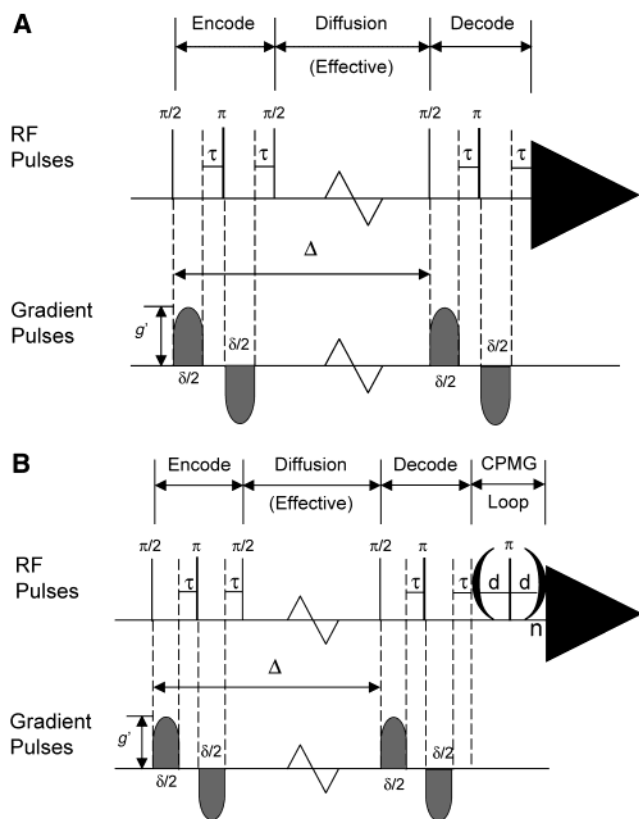


Figure 1. (A) BPPSTE pulse scheme employed for NMR diffusion measurements. Narrow and thick bars represent $\pi/2$ (90°) and π (180°) rf pulses, respectively. Sine bells represent the magnetic field gradient pulses of width $\delta/2$ and amplitude g' . The delays τ and Δ are the gradient recovery time and diffusion period, respectively. (B) BPPSTE-CPMG pulse sequence used to suppress protein signals. The CPMG pulse train consists of a series of 180° pulses separated by a short delay, d , with the total length of the pulse train ($2dn$) optimized to provide selective elimination of the protein resonances.

Typically, an excess of ligand is used to probe ligand–target interactions, so that ligand signals can be exclusively monitored to explore molecular binding events. Under these conditions, the observed diffusion coefficient (D_{obs}) reflects an average of the free (D_{free}) and bound (D_{bound}) states

$$D_{\text{obs}} = f_{\text{free}} D_{\text{free}} + f_{\text{bound}} D_{\text{bound}} \quad (2)$$

where f_{free} and f_{bound} are the mole fractions of free and bound ligand, respectively.

Diffusion experiments store the “encoded” magnetization in the longitudinal direction during the diffusion time (in stimulated echo-based experiments). Many other processes besides translational diffusion such as spin relaxation,^{12,13} chemical exchange,^{14–16} and cross-relaxation¹⁷ occur during this period and may become significant when ligand–target interactions are examined. In the

fast-exchanging system, signal losses due to T_1 relaxation should be constant, since the diffusion time remains fixed throughout the experiment. The effects of chemical exchange on NMR diffusion measurements have been extensively examined and can be minimized by optimizing experimental parameters and through using pulse sequences that incorporate bipolar gradient pulse pairs, like those shown in Figure 1.^{15,16,18,19}

In contrast, the influence of cross-relaxation on the results of NMR diffusion measurements, the subject of a recent publication,¹⁷ has been less thoroughly examined. Cross-relaxation between protons, also known as the nuclear Overhauser effect (NOE), is caused by dipolar relaxation between nuclei within 5 Å of each other.^{20–22} In situations involving ligand–protein binding equilibria, the NOEs that develop at the binding site can be transferred to the free ligand due to dissociation of the ligand–receptor complex.^{23–25} Ideally this transferred NOE (trNOE) can facilitate the determination of the bound ligand conformation.²⁶ In the present paper, the impact of trNOEs on NMR diffusion results is exemplified by measurements for ligands binding to HSA or dihydrofolate reductase (DHFR). The characterization of this effect for various molecular functionalities reveals specific details about the molecular nature of ligand–receptor interactions and thus provides useful information for drug screening.

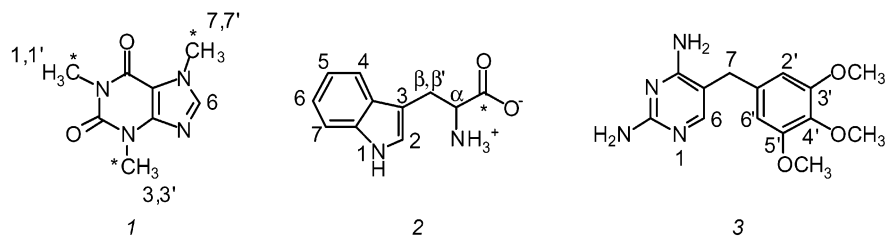
EXPERIMENTAL SECTION

Reagents and Materials. Trimethoprim (4.2 mM, Sigma, St. Louis, MO) with 120 mM DHFR (EC 1.5.1.3) was prepared in 25 mM phosphate buffer (pD 7.5). The DHFR (isolated from bovine liver) was purchased from Sigma and dialyzed with the buffer before use. Partially ^{13}C -enriched (99%) L-tryptophan and caffeine were obtained from Cambridge Isotope Laboratories, Inc. (Cambridge, MA). Chart 1 shows the structures and positions of the ^{13}C labels. The caffeine was analyzed at 10 mM in the presence of 150 μM HSA (Sigma). In addition, unlabeled L-tryptophan (Fluka, Milwaukee, WI) was analyzed at 5 mM in 75 μM HSA. The buffer was the same for all solutions except caffeine, which was analyzed in 25 mM phosphate buffer, pD 7.63. This buffer was prepared in D_2O and lyophilized to exchange hydrogen for deuterium prior to reconstitution in fresh D_2O , to reduce the intensity of the HOD resonance in the final solutions.

NMR Spectroscopy. The TMP and L-tryptophan samples were analyzed with a Bruker spectrometer operating at 599.13 MHz for ^1H observation using a 5-mm inverse triple-resonance ($^1\text{H}/^{13}\text{C}/^{15}\text{N}$) probe equipped with triple-axis actively shielded gradients. The z -gradient was calibrated at 298.2 K with a Bruker standard homogeneity HOD sample containing 0.1 mg/mL GdCl_3 . The maximum z -gradient amplitude was 76.3 G/cm. ^1H experiments for caffeine were conducted with a Bruker DRX

- (12) Lin, M.; Larive, C. K. *Anal. Biochem.* **1995**, *229*, 214–220.
- (13) Dixon, A. M.; Larive, C. K. *Appl. Spectrosc.* **1999**, *53*, 426A–440A.
- (14) Johnson, C. S., Jr. *J. Magn. Reson., Ser. A* **1993**, *102*, 214–218.
- (15) Moonen, C. T. W.; Van Gelderen, P.; Vuister, G. W.; Van Zijl, P. C. M. *J. Magn. Reson.* **1992**, *97*, 419–425.
- (16) Chen, A.; Johnson, C. S., Jr.; Lin, M.; Shapiro, M. J. *J. Am. Chem. Soc.* **1998**, *120*, 9094–9095.
- (17) Chen, A.; Shapiro, M. J. *Am. Chem. Soc.* **1999**, *121*, 5338–5339.
- (18) Peschier, L. J. C.; Bouwstra, J. A.; de Bleyser, J.; Junginger, H. E.; Leyte, J. C. *J. Magn. Reson., Ser. B* **1996**, *110*, 150–157.
- (19) Derrick, T. S.; Lucas, L. H.; Dimicoli, J. L.; Larive, C. K. *Magn. Reson. Chem.* **2002**, *40*, S98–S105.
- (20) Overhauser, A. W. *Phys. Rev.* **1953**, *89*, 689–700.
- (21) Overhauser, A. W. *Phys. Rev.* **1953**, *92*, 411–415.
- (22) Solomon, I. *Phys. Rev.* **1955**, *99*, 559–565.
- (23) Balaram, P.; Bothner-By, A. A.; Dadok, J. J. *Am. Chem. Soc.* **1972**, *94*, 4015–4016.
- (24) Neuhaus, D.; Williamson, M. P. *The Nuclear Overhauser Effect in Structural and Conformational Analysis*; VCH Publishers: New York, 1989.
- (25) Clore, G. M.; Gronenborn, A. M. *J. Magn. Reson.* **1983**, *53*, 423–442.
- (26) Mayer, M.; Meyer, B. *J. Med. Chem.* **2000**, *43*, 2093–2099.

Chart 1. Caffeine (1), L-Tryptophan (2), and Trimethoprim (TMP, 3)^a



^a The ¹³C isotopic labels are indicated by *.

spectrometer (500.13 MHz ¹H frequency) using a similar probe with a *z*-gradient coil constant of 65.3 G/cm. ¹³C experiments for caffeine were acquired with a 5-mm broadband observe probe (coil constant of 54.6 G/cm), because of its greater sensitivity for this nucleus. The temperature of the experiments was regulated at 288.2 and 298 K for the DHFR and HSA samples, respectively, using a Bruker B-VT regulator. The volume of the caffeine–HSA sample was constrained to the active volume of the probes using 5-mm NMR tube susceptibility matched for D₂O (Shigemi, Allison Park, PA).

The bipolar pulse pair longitudinal eddy current delay (BP-LED)⁸ pulse sequence was used for the ¹³C diffusion measurements of caffeine, employing a 15-ms delay to allow residual eddy currents to decay. To measure ¹H diffusion coefficients, the BPPSTE pulse sequence was used, which is effectively equivalent to BPLED without the eddy current delay.²⁷ Sixteen increments were obtained for each diffusion experiment, with the sine bell gradients varied linearly in amplitude, ranging from 2 to 95% of the calibrated maximum. For the caffeine ¹H measurements, the gradient range was optimized to obtain more points on the diffusion curves. The ¹H spectra were acquired into 16 384 data points with the carrier frequency set on the solvent resonance. When ¹³C spectra were collected, the number of data points, scans, and the spectral window were adjusted to optimize the signal-to-noise (S/N) ratio. The FIDs were apodized with 1 (¹H) or 5 (¹³C) Hz line broadening and zero-filled by a factor of 2 prior to Fourier transformation.

Diffusion Coefficient Analysis. NMR spectral data were analyzed using XWIN NMR 3.0 (Bruker), which utilizes a nonlinear least-squares algorithm to determine diffusion coefficients. A modified version of eq 1 was used, which scales the gradient amplitudes by a factor of $2/\pi$, to describe the amplitudes of the sine bell-shaped gradient pulses (*g*). A similar algorithm was used independently (Scientist, MicroMath, Inc., Salt Lake City, UT) for determination of L-tryptophan and TMP diffusion coefficients. Peak heights were utilized in the analyses. When the experimental conditions were such that S/N was poor (e.g., very high gradient amplitude or diffusion delay time), the spectra were carefully examined to include only clearly identified peaks in the analysis. Graphical data displays were created using Origin 7.0 (Microcal Software, Inc., Northampton, MA).

RESULTS AND DISCUSSION

As described previously, NMR diffusion measurements for benzoic acid binding to HSA revealed deviations from the expected single-exponential decay of ligand resonance intensity when long

diffusion delays (Δ) were used in the BPLED pulse sequence.¹⁷ Single-exponential decays were observed under similar acquisition conditions for ¹H and ¹³C diffusion data measured for the nonbinding glucose molecule and for ¹³C results measured for benzoic acid. These results suggested NOE transfer from the protein as the source of the curvature of the benzoic acid ¹H diffusion plots.¹⁷ However, in these studies, no attempt was made to reduce or eliminate the spectral background produced by the protein, which can also contribute to nonlinearity of ¹H NMR diffusion data.²⁸

To explore this phenomenon further, the effects of NOE transfer on NMR diffusion results were examined for caffeine and L-tryptophan, which bind to HSA, and TMP, an inhibitor of DHFR. A diffusion experiment at $\Delta = 1053$ ms was acquired for 10 mM caffeine in 150 μ M HSA. The results, shown graphically in Figure 2A, reveal curvature in the diffusion plots for all of the caffeine resonances, which is especially noticeable at higher gradient amplitudes. The diffusion delay acts as an NOE mixing time, because the magnetization is stored in the longitudinal direction during this part of the BPPSTE experiment. Because of the high ligand/protein concentration ratio (66:1), the small amount of magnetization resulting from the trNOE makes a minor contribution to the intense ligand signals when a weak gradient pulse is applied. However, for high gradient amplitudes, the ligand resonance intensity is significantly reduced due to diffusion, and the trNOE makes a greater contribution to the measured intensity. This gradient editing of excess free ligand signal permits observation of trNOE, which will build up through cross-relaxation within the diffusion time window.

Because ¹³C-labeled caffeine was used in these experiments, two ¹H resonances are observed for each of the three methyl groups due to ¹H–¹³C *J*-coupling. It is interesting to note that the biggest difference observed in Figure 2A is between the H7 and H7' proton resonances, resonances that arise from ¹H–¹³C *J*-coupled protons on the *same* methyl group. However, it does not seem physically reasonable that the ¹³C-coupled protons of a methyl group should reflect different trNOE contributions from the protein. Although the protein diffusion coefficient is significantly less than the ligand's, the intensity of the protein resonances underlying ligand signals will also be affected by the gradient pulses according to eq 1, especially at long Δ values and high gradient amplitudes. Therefore, the contribution of the protein background to the measured resonance intensity will not be constant throughout the experiment, leading to deviations from the expected single-exponential decay for ligand signals. There-

(27) Otto, W. H.; Larive, C. K. *J. Magn. Reson.* **2001**, *153*, 273–276.

(28) Derrick, T. S.; McCord, E. F.; Larive, C. K. *J. Magn. Reson.* **2002**, *155*, 217–225.

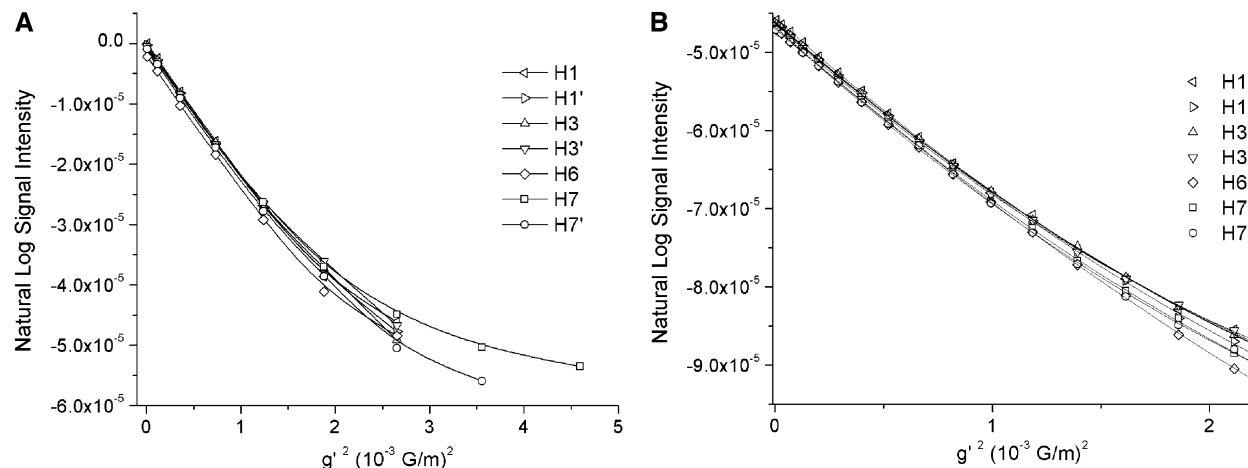


Figure 2. (A) ^1H diffusion data for 10.0 mM caffeine in the presence of 150 μM HSA at $\Delta = 1053$ ms acquired with the BPPSTE pulse sequence in the presence of the protein background. The gradient amplitudes ranged from 83.1 to 3950 G/m, and $\delta = 2.0$ ms. A B-spline function was used to connect the data points and illustrate the curvature. (B) ^1H diffusion data for the same sample acquired with the BPPSTE-CPMG pulse sequence to suppress the protein background and fit with a polynomial equation to illustrate curvature. The T_2 filter was 50 ms, and all other experimental conditions were the same as in (A). The ordinate values have been normalized by dividing the natural log of the signal intensities by $(\delta\gamma)^2(\Delta - \delta/3 - \tau/2)$.

fore, the protein background may confound attempts to observe curvature in NMR diffusion results produced by the trNOE.

To minimize the effect of the protein background on the measured ligand intensity, the standard BPPSTE pulse sequence was modified to eliminate the protein resonances by transverse (T_2) relaxation. Relaxation editing is an effective method for selectively attenuating the broad resonances of proteins widely used for the analysis of biological samples such as intact red blood cells and serum.^{29,30} The Carr–Purcell Meiboom–Gill (CPMG) pulse train^{31,32} can be incorporated into the BPPSTE pulse sequence following either the initial 90° excitation pulse²⁷ or the diffusion period.³³ Figure 1B shows the BPPSTE-CPMG pulse sequence used in this work with the T_2 filter incorporated after the diffusion period. The CPMG pulse train acts as a T_2 filter, selectively eliminating the protein signals and ensuring more accurate measurement of ligand resonance intensities.³⁴ To minimize the phase distortion caused by J -coupling modulation, the delay (d) between the 180° pulses of the CPMG train should be kept short and the length of the pulse train ($2dn$) optimized to achieve complete suppression of the protein signals.

The effectiveness of the CPMG pulse train in selectively removing the protein resonances is evident by comparing parts A and B of Figure 3. The spectral background produced by the HSA resonances is clearly visible in the BPPSTE spectrum, Figure 3A, even though the caffeine is present in a large molar excess. The Figure 3B spectrum appears to contain only a single component (caffeine) because the protein resonances have been eliminated by T_2 relaxation during the CPMG filter. The importance of eliminating the protein background in diffusion experiments can be readily discerned by examination of the diffusion

plot shown in Figure 2B obtained using the BPPSTE-CPMG pulse sequence. It is noteworthy that with this experiment the results obtained for the ^{13}C J -coupled proton pairs are now in good agreement. Although the curvature of the data plotted in this figure is much less than that observed in Figure 2A, these data were fit most effectively by a second-order polynomial rather than a linear equation. The curvature observed in Figure 2B results from negative NOE transfer from the protein to the ligand, which occurs when the magnetization is stored longitudinally during Δ , and could only be detected with certainty once the interference from the protein background was removed. This produces a positive intensity offset and is especially noticeable at higher gradient amplitudes.

The curvature observed in Figure 2B is different from the effects of cross-relaxation and chemical exchange that can result in oscillating signals as the gradient duration or diffusion time is increased. Recent work demonstrates that bipolar gradients

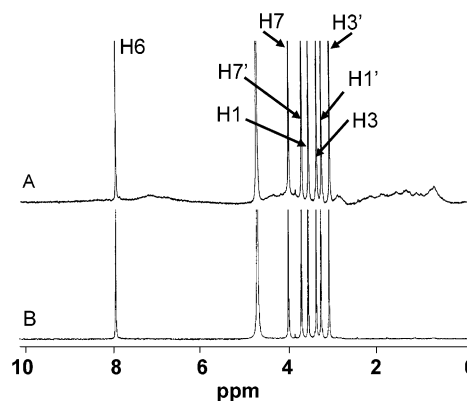


Figure 3. (A) ^1H BPPSTE spectrum measured for a solution of 10.0 mM caffeine in the presence of 150 μM HSA. The protein resonances are suppressed by T_2 filtering during the 50-ms CPMG pulse train, shown in the BPPSTE-CPMG spectrum in (B). Both spectra were acquired under the same gradient conditions ($g' = 83.1$ G/m, $\delta = 2.0$ ms) and included diffusion delay times of 104.2 (A) and 108.6 ms (B).

(29) Liu, M.; Nicholson, J. K.; Lindon, J. C. *Anal. Chem.* **1996**, *68*, 3370–3376.

(30) Rabenstein, D. L.; Millis, K. K.; Strauss, E. J. *Anal. Chem.* **1988**, *60*, 1380A–1391A.

(31) Carr, H. Y.; Purcell, E. M. *Phys. Rev.* **1954**, *94*, 630–638.

(32) Meiboom, S.; Gill, D. *Rev. Sci. Instrum.* **1958**, *29*, 688–691.

(33) Chin, J.; Chen, A.; Shapiro, M. J. *J. Comb. Chem.* **2000**, *2*, 293–296.

(34) Zhang, X.; Li, C. G.; Ye, C. H.; Liu, M. L. *Anal. Chem.* **2001**, *73*, 3528–3534.

suppress the oscillatory modulation due to these effects.^{16,19,35} The fact that curvature is observed for caffeine when its diffusion is measured with bipolar gradient pulses is additional evidence for a real trNOE from HSA to caffeine. In addition, it is conceivable that increasing Δ values could traverse the limit from fast to slow chemical exchange. This would theoretically be observed as a transition from a linear diffusion plot for small values of Δ to biexponential diffusion plots when Δ is long relative to the binding kinetics.⁴ However, excessive line broadening of the protein-bound ligand resonances would likely prevent detection of biexponential diffusion behavior. Even if biexponential diffusion behavior could be detected at long Δ values as a result of slow exchange on the diffusion time scale, the same behavior would be expected for all of the ligand protons; therefore, it cannot explain the differential curvature attributed to trNOE.^{17,36}

Although the trNOE effect can be observed for the caffeine–HSA system once the protein background is removed, it is only a slight effect for this ligand. Moreover, large differences are not observed between the caffeine protons, pointing to a relatively nonspecific interaction with albumin. Fluorescence quenching studies³⁷ and competition experiments involving caffeine's deuterated isotopomers³⁸ indicated that caffeine interacts with the single L-tryptophan residue in HSA and that all three methyl groups are important for binding. The dissociation constant is in the millimolar range, indicating relatively weak binding. Additional studies suggested two independent classes of binding sites, with K_d values in the 0.1–1.0 mM range.³⁹ Therefore, the results observed in Figure 2B may represent an average of the various binding interactions.

To determine the conformation of a ligand at the protein binding site, differential trNOE must be observed for specific ligand resonances.⁴⁰ Trimethoprim (TMP) is an antimalarial agent with high specificity for bacterial DHFR, an enzyme involved in generating tetrahydrofolate, which is an important cofactor in purine and amino acid synthesis. TMP–DHFR binding is very strong in the bacterial enzyme, with a K_d of 5.0×10^{-8} M.⁴¹ The interaction of TMP with bovine liver DHFR, used in this study, is somewhat weaker but still in the micromolar K_d range.⁴² Furthermore, the nature of TMP–DHFR binding has been thoroughly characterized through crystallographic studies.⁴³ The entire molecule is held in an interior cleft of the protein via hydrogen bonding and van der Waals interactions.

Although the molecular weight of TMP is similar to the other ligands studied, its diffusion coefficient ($(2.16 \pm 0.01) \times 10^{-10}$ m²/s at $\Delta = 20$ ms, $\delta = 5.0$ ms) is much slower due to the almost perpendicular orientation of the two aromatic rings and the

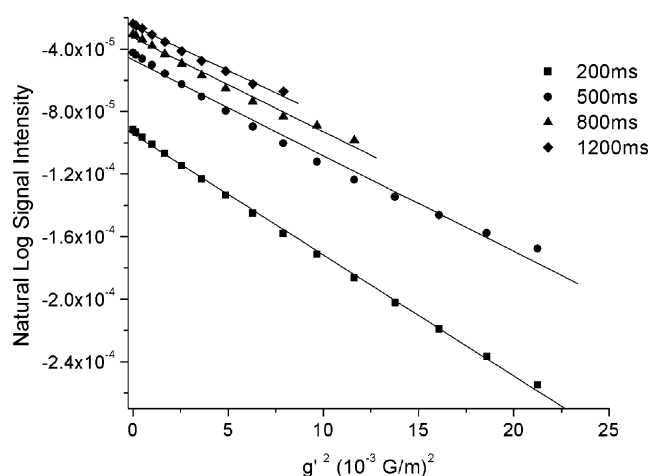


Figure 4. Diffusion data for H7 (3.52 ppm) of 4.2 mM TMP in the presence of 120 μ M DHFR as a function of Δ , shown with best linear fits of the data. Data were recorded with BPPSTE-CPMG, setting $\delta = 2.0$ ms, the total length of T_2 filter 32.9 ms, and varying g' from 97.1 to 4610 G/m. The diffusion time Δ changed from 200 to 1200 ms. The ordinate values have been normalized as in Figure 2.

corresponding geometries of the methoxy groups.⁴³ A plot similar to the one shown in Figure 2B was generated for all of the TMP ¹H resonances (not shown). Because the whole TMP molecule is held tightly in a deep binding pocket of the protein, the diffusion plots for all of the aromatic proton resonances were affected to a similar degree. However, the diffusion data for H7 demonstrated a slightly more pronounced curvature. Detection of the trNOE for H7 is especially significant since this proton is an isolated spin and therefore is less likely to experience trNOE via spin diffusion from other nearby protons on TMP. The greater curvature observed for H7 is not surprising, considering that the bond angles around this methylene group determine the conformation of TMP and thus its ability to position the molecule at the binding site.

Figure 4 depicts the diffusion results obtained with the BPPSTE-CPMG pulse sequence for the H7 proton of TMP as a function of Δ . Linear fits are shown for reference in Figure 4, and the poorest linear fits of the data are observed at the intermediate diffusion delay times. Interestingly, this result is in contrast to the previous report, where the trNOE was most readily detected at the longest Δ value. This is likely due to the presence of the protein background, which was not rigorously eliminated in those experiments.¹⁷ The reduction in the amount of curvature observed in Figure 4 for the longest Δ value may be due to the greater losses due to T_1 relaxation during the mixing period, which suppress the trNOE contribution. Similar results may be observed in many traditional transferred NOE experiments where the maximum in the buildup curve is often observed for mixing times in the 500-ms range,⁴⁴ although the buildup curve may depend on the amount of excess ligand used as well as the ligand T_1 relaxation time.²⁶

Although trNOE-induced curvature in the diffusion results obtained for caffeine and TMP did not reveal pronounced differences in the extent of protein interactions for the various ligand protons, this effect should be useful for characterizing which ligand functional groups interact most strongly with the protein.

(35) Dvinskikh, S. V.; Furó, I. *J. Magn. Reson.* **2000**, *146*, 283–289.

(36) Yan, J.; Kline, A. D.; Mo, H.; Zartler, E. R.; Shapiro, M. J. *J. Am. Chem. Soc.* **2002**, *124*, 9984–9985.

(37) González-Jiménez, J.; Frutos, G.; Cayre, I. *Biochem. Pharmacol.* **1992**, *44*, 824–826.

(38) Cherrah, Y.; Falconnet, J. B.; Desage, M.; Brazier, J. L.; Zini, R.; Tillment, J. P. *Biomed. Environ. Mass Spectrom.* **1987**, *14*, 653–657.

(39) Inestal, J. J.; González-Velasco, F.; Ceballos, A. *J. Chem. Educ.* **1994**, *71*, A297–A300.

(40) Balaram, P.; Bothner-By, A. A.; Dadok, J. *J. Am. Chem. Soc.* **1972**, *94*, 4017–4018.

(41) Feeney, J. *Angew. Chem., Int. Ed.* **2000**, *39*, 290–312.

(42) Sasso, S. P.; Gilli, R. M.; Sari, J. C.; Rimet, O. S.; Briand, C. M. *Biochim. Biophys. Acta* **1994**, *1207*, 74–79.

(43) Li, R.; Sirawaraporn, R.; Chitnumsub, P.; Sirawaraporn, W.; Wooden, J.; Athappilly, F.; Turley, S.; Hol, W. G. *J. Mol. Biol.* **2000**, *295*, 307–323.

(44) Chen, A.; Shapiro, M. *J. Am. Chem. Soc.* **1998**, *120*, 10258–10259.

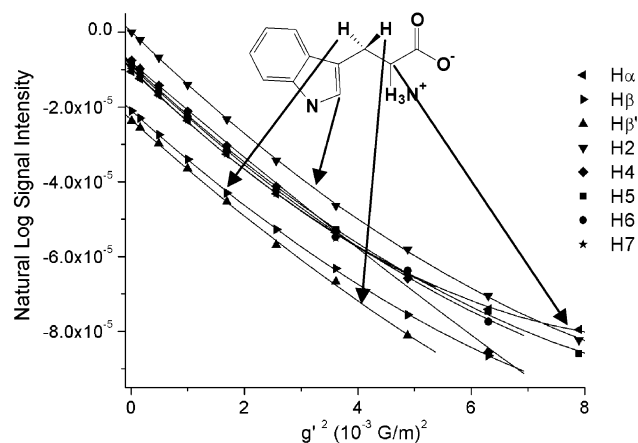


Figure 5. ^1H epitope map for 5.0 mM L-tryptophan in the presence of 75 μM HSA. Data were recorded with the BPPSTE-CPMG pulse sequence, where $\Delta = 800$ ms, $\delta = 2.0$ ms, g' ranged from 97.1 to 4610 G/m, and the total length of T_2 filter was 32.9 ms. Each data set was fit to a quadratic equation. The ordinate values have been normalized as in Figure 2.

To explore this effect further, similar measurements were performed for solutions containing L-tryptophan and HSA. L-Tryptophan is known to interact more strongly with HSA than caffeine, having a dissociation constant 10 times smaller.⁴⁵ Because the trNOE depends on close intermolecular interactions, it may be more pronounced when the affinity of the protein for the ligand is greater, as is the case for L-tryptophan, rather than for weak and nonspecific binding demonstrated by caffeine. The diffusion data acquired for L-tryptophan in the presence of the protein at $\Delta = 800$ ms are shown in Figure 5. The results obtained for $\text{H}\alpha$, $\text{H}\beta$, $\text{H}\beta'$, and $\text{H}2$ show the greatest degrees of curvature at high gradient amplitudes. The electrostatic interactions of the termini at the binding site anchor the ligand, facilitating interactions involving these protons. This model is consistent with one of the earliest reports of L-tryptophan/HSA interactions, where binding with tryptophan analogues confirmed the significance of the indole methylene group (β protons) and a "close fit" of the α -proton at a single binding site.⁴⁶ The similar degrees of curvature observed in the diffusion data for the phenyl protons ($\text{H}4$, $\text{H}5$, $\text{H}6$, $\text{H}7$) and the greater curvature for the $\text{H}\alpha$, $\text{H}\beta$, $\text{H}\beta'$, and $\text{H}2$ therefore reveals the binding specificity of HSA for L-tryptophan. Such epitope mapping is useful for describing structure–activity relationships and is being further developed by our group for potential applications in drug screening.³⁶ The advantages of using diffusion-based measurements rather than performing the more traditional trNOE experiments include reduced experimental times and selectivity against nonbinding ligands by the use of magnetic field gradients.

The trNOE influence on diffusion measurements seems to manifest itself in an unexpected way relative to a typical trNOE observed in a two-dimensional (2D) experiment. This work shows that trNOE is most readily observed at longer diffusion delay (mixing) times and for stronger binding associations. In the 2D NOESY experiment, spin diffusion may become significant at longer mixing times and obscure observation of trNOE. A stronger

ligand affinity may reduce the extent of exchange between free and bound states, thus also reducing the trNOE. In the systems studied herein, the ligand is in fast chemical exchange between free and bound states, as evidenced by a single set of resonances in the diffusion spectrum representing the average between those two states. Because the ligand excess is large in these studies, the intensity of the ligand resonances at low mixing times is largely representative of the free ligand. The NOE signal transferred from the limited amount of bound ligand is diluted by the large excess of free ligand, and the overall influence on the measured signal intensity is not significant. A longer Δ (mixing time) is required in this method to selectively attenuate the resonances of the free ligand so that the trNOE becomes a significant factor in the measured signal intensity. In this way, selectivity by diffusion overcomes the resolution issues that prevent observation of trNOE at lower mixing times, as in the 2D NOESY experiment. Under these conditions, a slower off-rate should facilitate the trNOE (given that chemical exchange remains fast), because more ligand is effectively bound during Δ , allowing a more significant contribution to measured ligand intensity.

Effects of Δ on the Measured Diffusion Coefficient.

Because one of the major uses of NMR diffusion measurements is for the determination of ligand–protein binding constants,⁴⁷ it is instructive to examine the effect of Δ on the value of D_{obs} . As indicated by eq 2, D_{obs} can be related to the fraction of the free and bound ligand and, therefore, to the ligand–protein binding constant.²⁸ As shown in Figure 6A, when a small value of Δ is employed (108.6 ms, 10% of the average T_1 null of the caffeine resonances), highly linear diffusion plots are obtained for each caffeine resonance because the contribution from the trNOE is not significant. Diffusion is a molecular property; therefore, under these experimental conditions, the slopes of the lines and the diffusion coefficients determined from those lines (listed in Table 1) are equivalent for each proton in the molecule. Because these diffusion results are plotted as normalized signal intensity versus the square of the gradient amplitude, the lines obtained at this short value of Δ are not only linear but they are collinear as demonstrated in Figure 6B. Therefore, diffusion measurements made for any proton should reflect the overall average state of the ligand and equivalent values of D_{obs} are expected for each resonance.

When excess ligand is used and Δ is kept short, the free ligand signals dominate the measured resonance intensities, and the value of D_{obs} ($(6.32 \pm 0.01) \times 10^{-10} \text{ m}^2/\text{s}$ at $\Delta = 108.6$ ms, $\delta = 2.0$ ms) is close to that measured for the free ligand ($D_f = (7.06 \pm 0.04) \times 10^{-10} \text{ m}^2/\text{s}$). The decrease in D_{obs} indicates that binding is occurring. The diffusion coefficients reported in Table 1 for caffeine were obtained by a nonlinear least-squares fit of the experimental data points to eq 1, even though slight curvature is observed at longer Δ values in the presence of the protein. The diffusion measurements for caffeine with and without protein were made under the same experimental conditions except the free caffeine was analyzed at 5.0 mM due to significant self-aggregation at higher concentrations, which is disrupted when the protein is added.⁴⁸

(45) Yang, Y.; Hage, D. S. *J. Chromatogr.* **1993**, *645*, 241–250.

(46) McMenamy, R. H.; Oncley, J. L. *J. Biol. Chem.* **1958**, *233*, 1437–1447.

(47) Fielding, L. *Tetrahedron* **2000**, *56*, 6151–6170.

(48) Rymdén, R.; Ståls, P. *Biophys. Chem.* **1985**, *21*, 145–156.

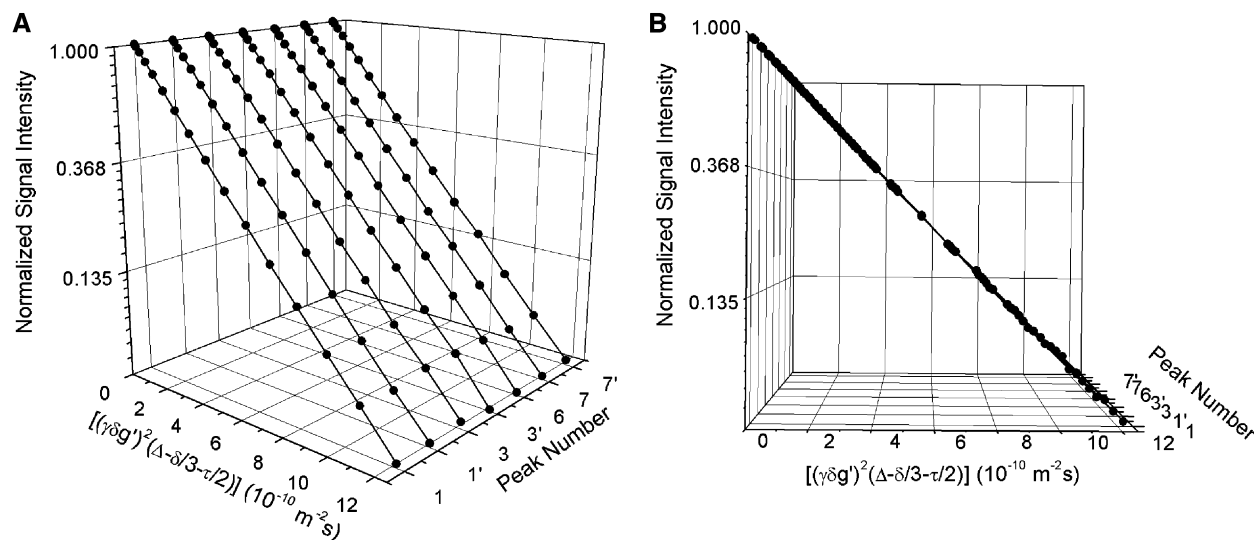


Figure 6. ^1H diffusion data for 10.0 mM caffeine in the presence of 150 μM HSA at $\Delta = 108.6$ ms (A). (B) Rotation of (A) to show the collinearity of the data, illustrating that diffusion is a molecular property. Data were acquired under the same conditions listed for Figure 3, and the ordinate values have been normalized by dividing by the signal intensity obtained when the lowest gradient amplitude is applied.

Table 1. ^1H Diffusion Coefficients (m^2/s) for 10.0 mM Caffeine without (Free) and with 150 μM HSA as a Function of Δ^a

peak/ Δ	108.6 ms (free) ^b	1053 ms (free) ^b	108.6 ms	266 ms	528.4 ms	791.3 ms	1053 ms
H1	7.07×10^{-10}	7.18×10^{-10}	6.32×10^{-10}	6.27×10^{-10}	6.03×10^{-10}	5.90×10^{-10}	5.72×10^{-10}
H1'	7.08×10^{-10}	7.19×10^{-10}	6.34×10^{-10}	6.27×10^{-10}	6.02×10^{-10}	5.89×10^{-10}	5.72×10^{-10}
H3	7.07×10^{-10}	7.18×10^{-10}	6.32×10^{-10}	6.24×10^{-10}	5.97×10^{-10}	5.84×10^{-10}	5.62×10^{-10}
H3'	7.08×10^{-10}	7.17×10^{-10}	6.31×10^{-10}	6.23×10^{-10}	5.97×10^{-10}	5.83×10^{-10}	5.62×10^{-10}
H6	6.98×10^{-10}	7.07×10^{-10}	6.30×10^{-10}	6.25×10^{-10}	6.04×10^{-10}	5.99×10^{-10}	5.82×10^{-10}
H7	7.07×10^{-10}	7.15×10^{-10}	6.33×10^{-10}	6.26×10^{-10}	6.05×10^{-10}	5.93×10^{-10}	5.75×10^{-10}
H7'	7.07×10^{-10}	7.16×10^{-10}	6.33×10^{-10}	6.28×10^{-10}	6.06×10^{-10}	5.98×10^{-10}	5.79×10^{-10}
average	7.06×10^{-10}	7.16×10^{-10}	6.32×10^{-10}	6.26×10^{-10}	6.02×10^{-10}	5.91×10^{-10}	5.72×10^{-10}
SD	3.78×10^{-12}	4.06×10^{-12}	1.16×10^{-12}	1.82×10^{-12}	3.68×10^{-12}	6.20×10^{-12}	7.81×10^{-12}
RSD, %	0.54	0.57	0.18	0.29	0.61	1.05	1.36

^a Data were acquired with $\delta = 2.0$ ms and g' varying from 83.1 to 3950 ($\Delta = 108.6$, 266 ms), 2290 ($\Delta = 528.4$ ms), 1660 ($\Delta = 791.3$ ms), and 1450 G/m ($\Delta = 1053$ ms). Reported values represent the average of two experimental trials. SD, standard deviation; RSD, relative standard deviation.

^b Due to significant self-aggregation of caffeine,⁴⁸ diffusion coefficients for the free ligand were measured at 5.0 mM.

At longer Δ values, the intensity due to the faster diffusing free ligand will be selectively attenuated, resulting in artificially reduced values of D_{obs} . In addition, longer values of Δ also produce positive curvature in the diffusion plots resulting from the trNOE. Therefore, when longer values of the diffusion delay are employed, the measured resonance intensities will be skewed preferentially, reflecting the properties of ligands that have been bound sometime during Δ . This is evidenced in Table 1 by the regular decrease in the values of D_{obs} determined as Δ is increased for caffeine in the presence of HSA. In contrast, the diffusion coefficients for caffeine alone are in good agreement at low and high Δ values. Furthermore, the results for caffeine imply that eq 2 does not strictly hold for all protons under the Δ range tested. Even for weakly binding ligands, significant errors in the resulting dissociation constant will occur when longer values of Δ are employed. Therefore, diffusion measurements used to determine equilibrium constants should be made at low Δ values to avoid discriminating against the fraction of free ligand and errors resulting from the trNOE.

Table 2 shows the ^{13}C diffusion coefficients for caffeine at low and high Δ values, which were again selected on the basis of the

Table 2. ^{13}C Diffusion Coefficients (m^2/s) for 10.0 mM Caffeine in 150 μM HSA^a

peak/ Δ	307.3 ms	768.3 ms	% decrease
C1	6.68×10^{-10}	5.71×10^{-10}	14.5
C3	6.68×10^{-10}	5.67×10^{-10}	15.1
C7	6.70×10^{-10}	5.73×10^{-10}	14.5
average	6.68×10^{-10}	5.70×10^{-10}	14.7
SD	1.17×10^{-12}	3.16×10^{-12}	n/a
RSD, %	0.18	0.55	n/a

^a SD, standard deviation; RSD, relative standard deviation; n/a, not applicable.

(^{13}C) T_1 relaxation time. At $\Delta = 307.3$ ms, the average ^{13}C diffusion coefficient for caffeine was higher than that determined by ^1H measurements at $\Delta = 266$ ms ($(6.68 \pm 0.01) \times 10^{-10} \text{ m}^2/\text{s}$ versus $(6.26 \pm 0.02) \times 10^{-10} \text{ m}^2/\text{s}$). This discrepancy is likely due to the errors in the coil constant calibrations and the inherently lower sensitivity of this nucleus relative to ^1H . The decrease in diffusion coefficients over the range of Δ values studied is on the same order as that observed for ^1H and occurs within approximately

Table 3. ^1H Diffusion Coefficients (m^2/s) for 4.2 mM TMP (H7) without (Free) and with 120 μM DHFR as a Function of Δ

peak/ Δ	20 ms	200 ms	500 ms	800 ms	1200 ms	% decrease
H7 (free)	2.16×10^{-10}	2.12×10^{-10}	2.13×10^{-10}	2.12×10^{-10}	2.05×10^{-10}	n/a ^a
H7	2.18×10^{-10}	2.07×10^{-10}	1.92×10^{-10}	1.87×10^{-10}	1.71×10^{-10}	21.6

^a n/a, not applicable.

the same time range. Thus, the experimental editing of free ligand is consistent, and the measured resonance intensities will be skewed, reflecting greater contributions from ligands that have been bound sometime during Δ . More importantly, perhaps, is that the data (not shown) did not demonstrate curvature ($R^2 \geq 0.998$ for a linear fit of the data for each carbon). This is expected for a nucleus whose gyromagnetic ratio is too small to be affected by the trNOE and agrees with the previous results.¹⁷ Therefore, observed curvature in the ^1H detected experiments can be attributed to trNOE from the protein to the ligand.

Because the fraction of bound ligand also depends on the value of the ligand–protein dissociation constant, the errors in D_{obs} encountered at longer values of Δ should be more pronounced for stronger binding ligands. Table 3 lists the diffusion coefficients determined as a function of Δ for the TMP H7 resonance intensities measured in the absence and presence of DHFR. The average diffusion coefficient determined for H7 in free TMP ($(2.16 \pm 0.01) \times 10^{-10} \text{ m}^2/\text{s}$) agrees within error with the average value for all protons measured at $\Delta = 20 \text{ ms}$ ($(2.18 \pm 0.01) \times 10^{-10} \text{ m}^2/\text{s}$). No significant curvature was observed in the diffusion plots at low or high Δ values, suggesting that intramolecular NOE is not contributing to any curvature that may be observed in the presence of the protein. When the protein is added, however, the diffusion coefficient of this proton decreases by 22% as Δ is varied from 200 to 1200 ms. This decrease is more than double that observed for caffeine and may be related to the approximate 2-fold difference in the ligand/protein concentration ratio in the TMP experiments as well as the much stronger binding constant. Screens of drug candidates for binding to a protein receptor often target ligands with K_d values in the nanomolar range. These results suggest that binding constants determined by NMR diffusion measurements for such strongly interacting ligands should be interpreted with caution, since the errors in D_{obs} induced by discrimination against the free ligand and arising from the trNOE may be significant even for low (i.e., 50–100 ms) values of Δ .

CONCLUSIONS

In the case of ligand–protein binding, NMR diffusion results can be significantly affected by trNOE buildup during the diffusion delay period. Curvature in the linearized diffusion data, especially

at intermediate values of the diffusion delay, is the signature of this effect. This curvature results from the transfer of magnetization from the protein to the ligand leading to a positive intensity offset and a lower diffusion coefficient. The elimination of protein resonances in the NMR spectra is extremely important for accurately detecting the trNOE, because the protein background can also contribute to curved ligand diffusion plots, thus obscuring the results. The trNOE contribution to resonance intensity is most evident at intermediate values of the mixing time, Δ (500–800 ms), and for the highest gradient amplitudes where the resonance intensities are significantly biased toward those ligands that were bound at some point during the experiment. Because the trNOE depends on close intermolecular interactions, it is more pronounced when the ligand affinity is very strong ($K_d \sim \mu\text{M}$) rather than for weak and nonspecific binding. This effect offers a clear advantage over other diffusion-based NMR screening methodologies that can lead to false positives when a ligand binds nonspecifically to multiple binding sites. Differential degrees of curvature in the ligand diffusion results permit determination of binding specificity, and such epitope mapping is potentially useful for the screening of drug candidates. These results further suggest that quantitative NMR measurements of ligand binding affinity should be made only with short values of the diffusion delay time. Since accurate determination of ligand K_d values depends on knowing the true weighted average diffusion coefficient, diffusion NMR analysis at short diffusion delay times will minimize errors resulting from selective editing of the free ligand intensity as well as from the trNOE contribution.

ACKNOWLEDGMENT

L.H.L. gratefully acknowledges the financial support of NIH training grant 2 T32 GM08545 in the Dynamic Aspects of Chemical Biology and the technical support of Mr. Stephen Huhn at the Bruker Instruments Applications Laboratory, Billerica, MA. L.H.L. and C.K.L. acknowledge the NSF Grant CHE-9977422 for partial funding for the 500-MHz spectrometer used in this research.

Received for review September 11, 2002. Accepted November 14, 2002.

AC020563O